ELSEVIER

Catalysis Today 54 (1999) 267–282

CATALYSIS TODAY

www.elsevier.com/locate/cattod

Large scale studies in solar catalytic wastewater treatment

Ralf Dillert[c], Alberto E. Cassano[b], Roland Goslich[a], Detlef Bahnemann[a,*]

[a] *Institut für Solarenergieforschung GmbH Hameln/ Emmerthal, Sokelantstrasse 5, D-30165 Hannover, Germany*
[b] *INTEC (Universidad Nacional del Litoral, and CONICET), Güemes 3450, 3000 Santa Fe, Argentina*
[c] *Ecotransfair, Rebenring 33, D-33106 Braunschweig, Germany*

Abstract

The practical applicability of the double-skin sheet reactor (DSSR) for solar catalytic wastewater treatment has been checked at laboratory scale, in Hannover, and at the outdoor test-field of the Plataforma Solar de Almería (PSA), in Spain, using dichloro acetic acid (DCA) as the standard test pollutant. This type of photoreactor has also been successfully used for the treatment of biologically pretreated industrial wastewater on laboratory and pilot plant scale. To analyze the experimental results, a first-order rate law in concentration and radiation density flux (assumed constant for each run) has been derived: $R_V = k_3(A_R/V_R)\bar{q}_{UV}c$, where k_3 is a lump kinetic parameter, A_R is the illuminated reactor area, V_R is the volume of the photoreactor, $\bar{q}_{UV}$ is the time averaged radiation density flux of UV energy, and c is the concentration of the pollutant. It has been observed that the integrated form of this rate law fits fairly well the experimental data obtained with a model compound and solar energy, and that an expression derived from this rate can be used for an approximate scaling-up of a solar catalytic wastewater treatment plant. ©1999 Elsevier Science B.V. All rights reserved.

Keywords: Photocatalysis; Photoreactors; Titanium dioxide; UV radiation

1. Introduction

The pollution of surface and ground waters is a serious problem of industrial society. Therefore, it is very important to develop processes for cleaning up polluted aquifers, as well as to make them available for industrial facilities. Photocatalytic detoxification, employing titanium dioxide, TiO_2, is a promising method for this purpose [1,2].

The concept of photocatalytic degradation is simple: an electron/hole pair is generated in a semiconductor particle, provided that a photon with appropriate energy is absorbed. If these charge carriers reach the catalyst surface before recombination, they can be used for chemical reactions, i.e., for oxidation or reduction of pollutants.

Wavelengths shorter than 400 nm are essential for the excitation of TiO_2, at present the most suitable semiconducting material for photocatalysis. In the solar spectrum, the wavelength range that can be used for the excitation of TiO_2, i.e., the UV-A region between 300 and 400 nm, approximately 50 W m^{-2} radiation from the sun is reaching the surface of the earth under AM 1.5 conditions [3].

To ensure efficient conversion of incident photons to charge carriers, the appropriate design of a solar reactor is of utmost importance. For example, it has been reported that light concentrating systems, such as parabolic-trough reactors, do not necessarily exhibit advantages over non-light concentrating systems [4–8]. It is well known that in the wavelength range of the solar spectrum that can be used for the excitation of TiO_2, the diffuse and direct portion of the solar radiation (AM 1.5) reaching the surface of the

---

[*] Corresponding author.

0920-5861/99/$ – see front matter ©1999 Elsevier Science B.V. All rights reserved.
PII: S0920-5861(99)00188-1

earth are almost equal [3]. This means that a light concentrating system cannot employ much more than half of the solar radiation available for catalyst activation. Moreover, Brandi et al. [9] have also shown that, even under the most favorable operating conditions for a parabolic-trough reactor, its solar radiation collection efficiency cannot be larger than 70% of that corresponding to a flat-plate reactor of the same photon harvesting area.

In this paper, the attention will be focused on a new type of a non-light concentrating photoreactor, namely, the Plexiglas® double-skin sheet reactor (DSSR). The DSSR has been introduced recently [10–15], and is now available commercially (SolAcryl Gesellschaft für regenerative Energiesysteme GmbH, Elsenfeld, Germany). It consists of a flat and transparent structured box made of polymethylmethacrylate (Plexiglas®). The suspension containing the pollutant(s) and the photocatalyst is pumped through a meandering channel inside the reactor. Once the degradation process is completed, the suspended photocatalyst has to be removed from the liquid. This type of reactor can utilize both the direct and the diffuse portion of the solar radiation.

The practical applicability of this type of reactor has been checked at laboratory scale in Hannover [10] and at the outdoor test-field of the Plataforma Solar de Almería (PSA), in Spain [11,12], using dichloro acetic acid (DCA) as the standard test pollutant. Recently, the DSSR has also been used for treatment of biologically pretreated industrial wastewater at laboratory [13,14] and pilot plant scale [15].

A very simplified mathematical approach for the kinetic analysis of photocatalytic experiments is presented. Experimental results obtained with the DSSR, which have been published recently [10–15], are analyzed in terms of this method. The suitability of this model for an approximate scale-up of a solar catalytic wastewater treatment plant from laboratory-scale experiments is also discussed.

2. Kinetic analysis

To compare different photocatalytic experiments, often an apparent photonic efficiency ζ has been used in the literature [10].

$$\zeta = \frac{R_{\mathrm{V},0} V_{\mathrm{R}}}{A_{\mathrm{R}} \int_{\lambda} q_{\lambda} \mathrm{d}\lambda} \tag{1}$$

Eq. (1) is defined in terms of the initial photocatalytic degradation rate $R_{\mathrm{V},0}$ and the radiation density flux $\int_{\lambda} q_{\lambda} \mathrm{d}\lambda$ arriving at the photocatalytic reactor (in units of moles per Einstein). Apparent photonic efficiencies are useful for laboratory experiments, because, under these circumstances, the photon flux should be constant and well known, and very often the degradation rate can be determined by the slope of the concentration versus time profile. However, for comparing solar outdoor experiments under fluctuating radiation conditions, the photonic efficiency cannot be used in a straightforward manner.

Besides, photonic efficiency, reaction rate or a kinetic constant determined directly from the slope of the concentration–time profile do not provide enough information for scaling-up a solar catalytic wastewater treatment plant from laboratory-scale experiments. For this purpose, a useful kinetic approach has to include (i) the pollutant concentration or related variable (e.g., TOC, COD), (ii) the photon density flux reaching the reactor area, (iii) the total volume of the suspension to be treated, (iv) the light harvesting area, (v) the photoreactor volume, and (vi) the irradiation time as the minimum design variables.

Consider a typical degradation unit made of a solar-irradiated reactor (volume V_{R}) and a storage tank (volume V_{T}) forming the main parts of a batch recirculating system containing a total suspension volume V_{S}. When the reactor operates under low conversions per pass inside the loop of a well-mixed batch system, it can be shown that [16]

$$R_{\mathrm{V}} = -\frac{V_{\mathrm{S}}}{V_{\mathrm{R}}} \frac{\mathrm{d}c}{\mathrm{d}t} \tag{2}$$

where $\mathrm{d}c/\mathrm{d}t$ is the change in concentration measured in the tank. In photocatalytic water degradation systems, this equation will be more valid when the recirculating flow rate is high. This condition is usually accomplished to maintain uniform concentration of the catalyst throughout the water suspension. The real challenge when working with real wastewaters, and usually variable solar irradiation rates, is the formulation of the left-hand side of Eq. (2); particularly, if one tries to keep the mathematical complexity of the model in line with the type of information that will be available for its application.

In formulating R_V, two approximations will be made: (i) it is directly proportional to the volume and time averaged photon absorption rate $\langle\langle e^a\rangle_{V_R}\rangle_\tau$, and (ii) it is directly proportional to the concentration of the organic pollutant c (determined as total organic carbon, TOC, in this work).

$$R_V \cong k_1 \left\langle \langle e^a \rangle_{V_R} \right\rangle_\tau \; c \qquad (3)$$

The two approximations used in Eq. (3) are not always valid. First-order dependence with respect to the photonic absorption rate has been reported when the irradiation rate is low (below 1 sun is the order of magnitude usually referred to). First-order dependence with respect to the organic compound has been found usually at low pollutant concentrations (a limiting case of the more general apparent Langmuir–Hinshelwood (L–H) kinetics).

The volume averaged photon absorption rate is given by an additional simplification in terms of the photon density flux arriving at the reactor surface:

$$\langle e^a \rangle_{V_R} \cong \frac{A_R \int_\lambda \alpha_\lambda \, k^*_\lambda \, q_{UV,\lambda} \, d\lambda}{V_R} \qquad (4)$$

The dimensionless parameter α_λ ($\alpha_\lambda \leq 1$) is related to the ability of a reactor system to use the available light, and takes into account the losses of the photon energy due to scattering, reactor wall reflection and absorption, etc. Again, this assumption is only approximate because it does not consider variations of the photon absorption rate with the reactor depth. Additionally, scattering, as well as reactor wall reflection and absorption, can hardly be well modeled with a single constant.

We can further assume that the irradiation is pseudo-monochromatic (i.e., $k^*_\lambda \alpha_\lambda = k_2 \alpha$) and Eq. (4) can be rewritten as

$$\langle e^a \rangle_{V_R} \cong k_2 \, \alpha \, \frac{A_R}{V_R} \, q_{UV} \qquad (5)$$

In Eq. (5), k_2 is the value of k^*_λ for $\lambda = 350$ nm, and q_{UV} an average value over the wavelength range of the useful radiation density flux. Once again, this is an approximation. For the case of solar irradiation in the 300–400 nm range, the radiation density flux arriving at the surface of the reactor decreases when one moves towards the shorter wavelengths [3]. On the other hand, titanium dioxide absorption has just the opposite trend [17]. Thus, some form of compensation effect may be possible. Unfortunately, q_{UV} not only varies with wavelength, it is usually not constant along the day of a typical solar reactor operation [18,19]. Instead, an average value over the exposure time will be used. Then, the time and volume averaged photon absorption rate is given by

$$\left\langle \langle e^a \rangle_{V_R} \right\rangle_\tau = \frac{\int_\tau \langle e^a \rangle_{V_R} \mathrm{d}t}{\int_\tau \mathrm{d}t} \cong \frac{\sum_{i=1}^{n} \langle e^a \rangle_{V_R,i}}{n} \qquad (6)$$

or, after inserting Eq. (5), by

$$\left\langle \langle e^a \rangle_{V_R} \right\rangle_\tau = k_2 \, \alpha \, \frac{A_R}{V_R} \, \frac{\sum_{i=1}^{n} q_{UV,i}}{n} \qquad (7)$$

Substituting this expression into Eq. (3) yields the reaction rate per unit suspension volume:

$$R_V = k_1 \, k_2 \, \alpha \, \frac{A_R}{V_R} \, \frac{\sum_{i=1}^{n} q_{UV,i}}{n} \, c \qquad (8)$$

Inserting this result into Eq. (2), and using the abbreviations $k_3 = k_1 k_2 \alpha$ and $\bar{q}_{UV} = \frac{\sum_{i=1}^{n} q_{UV,i}}{n}$ finally yields the time rate of change of the pollutant concentration in the tank:

$$\frac{\mathrm{d}c}{\mathrm{d}t} = - \, k_3 \, \frac{A_R}{V_S} \, \bar{q}_{UV} \, c \qquad (9)$$

For constant radiation fluxes, Eq. (9) is equivalent to a first-order rate law in concentrations. After integration within the limits $c = c_0$ at time $t = 0$ and $c = c$ at time t, the usual exponential expression is obtained:

$$c = c_0 \exp \, - \left(k_3 \frac{A_R}{V_S} \, \bar{q}_{UV} \, t\right) \qquad (10)$$

Analogous expressions to Eqs. (9) and (10) have recently been derived by Sagawe [20], Sagawe et al. [21] and Bahnemann et al. [12], originating from similar assumptions.

Rearrangement of Eq. (10) yields an expression to calculate the kinetic parameter k_3:

$$k_3 = \frac{V_S}{A_R} \, \frac{1}{\bar{q}_{UV}} \, \frac{1}{t} \, \ln\left(\frac{c_0}{c}\right) \qquad (11)$$

Note that the kinetic parameter k_3 is not a true kinetic constant. On one hand, it was obtained under the following assumptions: (i) the reaction is first order with respect to the photon absorption rate; (ii) the reaction is first order with respect to the ‘pollutant’ concentration; (iii) for complex reaction mixtures, the pollutant concentration can be well represented by a single ‘composition’, indicated by the TOC; (iv) the radiation is pseudo-monochromatic; (v) a simplified expression is used for the time average of the reactor volume average photon absorption rate; (vi) the photon absorption rate is represented by the flux of arriving photons affected by a constant to account for all non-absorbed photons; and (vii) this constant is the same for all reactors, independent of wavelength. On the other, this very simple kinetic model does not take into account (i) the type of catalyst; (ii) the catalyst concentration; (iii) the molecular oxygen concentration in the reactor; (iv) pH effects; and (v) those effects on the reaction derived from the existence of impurities in the incoming stream of fluid.

This simplified model can be substantially improved provided that the experiments are carried out exclusively with model compounds and solar radiation simulators or solar illumination on some specially selected days. (See, for example, Alfano et al. [22] or Rossetti et al. [23]). However, our present knowledge in relation to these processes will lead us to an useless effort if one considers that solar fluxes are not constant — even in short time intervals — and real wastewaters have variable and very often not well-defined composition. Nevertheless, with many limitations, crude approximation, like the one presented here, may be useful for comparing performances of different solar photocatalytic reactors analyzed under equivalent operating conditions.

3. Experiments with dichloro acetic acid

3.1. Laboratory experiments

In the experiments performed using the DSSR, the degradation of dichloro acetic acid (DCA) in illuminated aqueous TiO_2 suspensions was investigated, varying the kind of the TiO_2 photocatalyst (Degussa P 25 or Sachtleben Hombikat UV 100), its concentration, and the content of molecular oxygen. DCA has been used to characterize and compare the performance of different types of solar reactors and photocatalysts in small-scale laboratory experiments and during several experimental periods at the PSA since 1992 [24–27]. DCA can be conveniently used since it has a very low vapor pressure and is soluble in water at any concentration. DCA is a relatively strong organic acid ($pK_A = 1.29$) and therefore present in its anionic form at all pH values employed. Moreover, DCA is also an environmentally relevant pollutant, as it can be found anywhere in nature today, because it is a non-biodegradable metabolite of different chlorinated substances, such as trichloroacetic acid, perchloroethylen and others [26]. The photocatalytic degradation of DCA in TiO_2 slurries obeys the following stoichiometry [26]:

$$\mathrm{CHCl_2COO^-} + \mathrm{O_2} \rightarrow 2\mathrm{CO_2} + \mathrm{H^+} + 2\mathrm{Cl^-} \qquad (12)$$

In the laboratory studies, an experimental setup was used, which consisted of a modified Plexiglas® double-skin sheet (SDP 16/32, Röhm GmbH, Darmstadt (Germany), length = 1400 mm, height = 980 mm, 30 interconnected channels of 28.5 mm × 12 mm) as the photoreactor and a reservoir (30 l) connected by PVC tubes. In all experiments, this system was operated in a recirculation mode. A centrifugal pump provided the flow of contaminated water. The flow rate was $11.8\,\mathrm{l\,min^{-1}}$, i.e., the residence time in the photochemical reactor was 87 s. This flow rate resulted in Reynolds numbers of about 9000; therefore, the flow conditions were turbulent.

In indoor experiments, the DSSR was illuminated by a custom-made illumination unit equipped with 16 fluorescent tubes (Cleo-Performance R 40 W, Phillips; $\lambda_{max} = 355\,\mathrm{nm}$). The illumination unit was aligned in parallel to the reactor surface at a distance of 2.5 cm. The illuminated reactor surface A_R was $125 \times 69\,\mathrm{cm^2}$ ($0.86\,\mathrm{m^2}$). It was irradiated with 5.9×10^{-3} mol photons per minute, as determined by ferrioxalate actinometry, corresponding to an area averaged, apparent energy density flux of $38.5\,\mathrm{W\,m^{-2}}$. The illuminated reaction volume V_R was 10.4 l, and the total volume of the suspension V_S varied between 20 and 30 l. Solar degradation experiments were performed in Hannover in the beginning of May 1995. For this purpose, the reactor was adjusted to an inclination angle of 45°. During the experiments, the whole surface of the reactor was irradiated by the sun ($A_R = 1.34\,\mathrm{m^2}$, $V_R = 14.4$ l, $V_S = 25$ l).

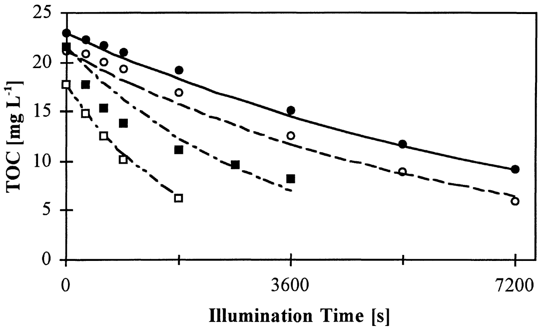

Fig. 1. TOC versus illumination time during the laboratory experiments of the photocatalytic degradation of DCA. The lines have been calculated using Eq. (10) and the data given in Table 1. (Experimental conditions: (–●——) 5.0 g l^{-1} P 25 (Run 14); (---○---) 5.0 g l^{-1} P 25, oxygenated suspension (Run 16); (–·–·–■·–) 7.5 g l^{-1} Hombikat UV 100 (Run 4); (–··–··□–··–··–) 7.5 g l^{-1} Hombikat UV 100, oxygenated suspension (Run 6).

The change of TOC versus illumination time in some typical experiments is shown in Fig. 1.

In all cases, an apparent first-order rate law with respect to the TOC 'hypothetical composition' can describe the rate of disappearance of the TOC. Similar results have been shown recently [24]. From the obtained experimental data and using a parameter estimator, k_3 can be calculated by application of Eq. (10). For each experiment, the initial degradation rate was calculated using Eq. (8) (with the initial DCA concentration), while the initial photonic efficiency ζ was calculated using Eq. (1).

Results for k_3 and ζ are presented in Table 1, together with the relevant experimental details.

With artificial light and when no oxidant was purposely added, photonic efficiencies varying between 0.03 and 0.12 were obtained, depending on the kind and concentration of the photocatalyst employed. The photocatalytic degradation of DCA was more effective with Sachtleben Hombikat UV 100, than with Degussa P 25 employed as photocatalyst, in good agreement with data from small-scale laboratory studies [27]. With both photocatalysts, and usually passing through a maximum, the efficiency increased with increasing catalyst concentration, as it has also been shown in laboratory experiments using a 50 ml stirred-tank reactor and artificial illumination [27]. It should be mentioned that, as should be expected, this increase is not linear with catalyst concentration. However, employing the DSSR, photonic efficiencies in aerated suspensions were lower (about 0.1 with Sachtleben Hombikat UV 100 and about 0.06 using Degussa P 25) than under idealized small-scale laboratory conditions, where photonic efficiencies up to 0.22 have been found using Hombikat UV 100 [27]. Qualitative measurements of the photon flux, with a luxmeter behind the reactor, have shown that a part of the incident UV light passed through the photoreactor when a photocatalyst concentration of 1 g l^{-1} was used. Also, it has been shown [28] that back-scattering losses may be very important in flat-plate reactors. Thus, these low photonic efficiencies, obtained in terms of apparent photon absorption rates, can at least partly be explained by an incomplete absorption of photons and the existence of higher reflection losses in the DSSR configuration (i.e., α is not the same for both reactor types).

Purging the suspension with molecular oxygen resulted in an increase in the photonic efficiencies. From this observation, it can be concluded that using the DSSR unit with a rather large reaction volume, there is a partial limitation in the DCA degradation rate by a depletion of molecular oxygen in some parts of the reactor space. Since these results have been obtained under turbulent flow conditions, one can safely say that oxygen concentration will be an important component in a more complete representation of real reacting systems. This is plausible since molecular oxygen is a reactant necessary for the photocatalytic degradation of DCA (Eq. (12)).

It has been reported that the photonic efficiency of the photocatalytic DCA degradation decreases considerably as the light intensity is increased [27]. Run No. 7 is a typical example of this behavior. Thus, the linear dependence for the photonic absorption rate cannot be extrapolated to very low irradiation rates.

Under illumination with artificial UV light, k_3 values between 5.5×10^{-8} and 42.9×10^{-8} $m^3 W^{-1} s^{-1}$ were obtained. The lines in Fig. 1 represent the exponential curve fits to the respective experimental data, calculated with the thus-derived k_3 values, according to the rate law given in Eq. (10). As can be seen from these plots, this rate law fits most of the experimental data fairly well.

As expected, the values of k_3 show the same dependencies as the values of the photonic efficiencies ζ, i.e., in all cases, the values of the kinetic parameter k_3 are significantly lower for Degussa P 25 when compared with Sachtleben Hombikat UV 100 for a given

Table 1
Experimental data and kinetic parameters (k_3) of the laboratory experiments of the photocatalytic degradation of dichloro acetic acid[a]

Run No.	Catalyst	c_{cat} (g l^{-1})	V_{s} (l)	Gas	TOC$_0$ (mg l^{-1})	$k_3 \times 10^8$ (m^3 W^{-1} s^{-1} V)	$\zeta \times 10^3$
1	Hombikat UV 100	1.0	25	–	21.5	7.4 ± 0.1	45
2	Hombikat UV 100	5.0	30	–	20.6	11.2 ± 0.7	66
3	Hombikat UV 100	5.0	30	–	22.1	9.5 ± 0.4	60
4	Hombikat UV 100	7.5	20	–	21.4	18.8 ± 1.6	115
5	Hombikat UV 100	7.5	25	air	17.3	20.6 ± 1.0	101
6	Hombikat UV 100	7.5	25	oxygen	17.7	42.9 ± 2.2	216
7[b]	Hombikat UV 100	7.5	25	–	12.7	77.5 ± 12.9	280
8	Hombikat UV 100	10.0	25	–	22.2	10.3 ± 0.9	65
9	Hombikat UV 100	10.0	25	–	22.3	8.5 ± 0.2	54
10	Hombikat UV 100	15.0	25	–	13.6	15.7 ± 1.9	61
11	Hombikat UV 100	15.0	25	–	13.3	7.0 ± 0.6	26
12	P 25	1.0	25	–	21.9	5.5 ± 0.2	34
13	P 25	2.5	25	–	19.6	7.6 ± 0.1	42
14	P 25	5.0	25	–	22.9	9.6 ± 0.2	63
15	P 25	5.0	25	air	22.6	10.1 ± 0.4	65
16	P 25	5.0	25	oxygen	21.0	12.3 ± 0.5	74

[a] Experimental conditions: DCA; pH 3; ambient temperature; $\bar{q}_{\mathrm{UV}} = 38.5\,\mathrm{W\,m^{-2}}$; $V_{\mathrm{R}} = 10.4\,\mathrm{l}$, $A_{\mathrm{R}} = 0.86\,\mathrm{m^2}$, $\dot{V} = 11.8\,\mathrm{l\,min^{-1}}$.

[b] Solar experiment; $\bar{q}_{\mathrm{UV}} = 17.2\,\mathrm{W\,m^{-2}}$ (Hannover, Germany, 4 May 1995, 2:00–6:00 p.m.); $V_{\mathrm{R}} = 14.4\,\mathrm{l}$; $A_{\mathrm{R}} = 1.34\,\mathrm{m^2}$; $\dot{V} = 11.8\,\mathrm{l\,min^{-1}}$.

catalyst concentration; they increase with increasing catalyst concentration and with increasing concentration of molecular oxygen present in the suspension. Run No. 7 gave a surprisingly high k_3 value. This is a result that was also observed in other experiments, reported below, when the radiation density flux was low, clearly contradicting the linear dependence included in the simplified model. However, no improvements were obtained using a kinetic expression with a square root dependence of the photonic efficiency on the radiation density flux being incorporated into it.

3.2. Field studies at the Plataforma Solar de Almería

During May 1996, solar experiments using the DSSR have been performed at the Plataforma Solar de Almería (PSA) in Spain [11,12]. The photocatalytic reactor setup used at the PSA consisted of two or three DSSRs connected in series, which were joined by PVC tubes to a reservoir. A DSSR consisted of a modified double-skin sheet (SDP 16/32), manufactured by the Röhm GmbH, Darmstadt. One photoreactor had a length of 1395 mm, a width of 950 mm, and contained 30 interconnected channels, each of which had an opening of 27 mm × 12 mm. The total illuminated volume of one DSSR added up to 13.6 l; the illuminated surface area was 1.33 m^2. During all experiments, the complete upper surface of the DSSRs was exposed to the sun. The inclination angle was adjusted to 37°, with the face of the reactor facing south. The suspension was recirculated by means of a centrifugal pump. The flow rate was adjusted to 12.0 l min^{-1}. In all experiments, the TiO$_2$ catalyst powder was added to the stock container without any additional treatment. The concentration of the photocatalyst was varied between 0.2 and 5 g l^{-1}. In a typical experiment with DCA being the model pollutant, its concentration was adjusted to 2.5 mmol l^{-1} (60 mg l^{-1} TOC) after the photocatalyst was added.

For comparison, the photocatalytic degradation of DCA was also investigated using a cascade of up to six compound parabolic collecting reactors (CPCR) in parallel experiments under identical experimental conditions. A CPCR is a trough reactor without light concentrating properties. It differs from a conventional parabolic-trough reactor by the shape of its reflecting mirrors. A reflector of a parabolic-trough reactor has a parabolic profile, with the reaction pipe in its focal line. Consequently, only direct, as opposite to diffuse, light entering the parabolic-trough can be focused into the reaction pipe, and a sun-tracking system is required. The shape of a CPCR's reflector usually consists of two half portions of parabolic cylinders set side by side. The reaction center is located close above the union of the two parabolic profiles.

This geometry enables light entering from almost any direction to be reflected into the 'center' of the CPCR, i.e., most of the diffuse light entering the module can also be employed for the photocatalytic reaction. Due to this geometry, a CPCR exhibits only a small concentration factor. (The CPCR installed at the PSA has a concentration factor of 1.15, i.e., this type of reactor has practically no light concentrating properties [29].) Moreover, due to its geometry, a CPCR must not necessarily track the sun. The azimuth should be adjusted to the complementary angle of the geographical altitude, and the pipes should be aligned south and perpendicular to the horizon.

At the PSA, two CPCR modules are joined together forming one CPCR unit [30,31]. Three units are connected in series, but each of it can be by-passed. The CPCRs used at the PSA were produced by the Industrial Solar Technology Corporation, Denver, CO, USA. One CPCR-module consists of eight parallel reflectors made from polished aluminum. A single reflector has a length of 1220 mm and a width of 152 mm, i.e., the effective light-harvesting area of one module, consisting of eight reflectors, adds up to 1.48 m^2. A reaction pipe, made of a transparent fluoro polymer (Teflon), is fixed at the 'center' of each CPC reflector, through which the suspension containing the photocatalyst and DCA as the model pollutant circulates. The reaction pipe is as long as the reflector (1220 mm), has an inner diameter of 48 mm, and, consequently, an illuminated volume of 2.21 l. The overall illuminated volume of one module adds up to 17.7 l. The connectors between the absorber pipes are made of polypropylene. The angle of incidence was adjusted to 37°. The suspension was recirculated by means of a centrifugal pump through the CPCR units and a tank with a flow rate of approximately 33.3 l min^{-1}. The tank and the connecting pipes (40 mm inner diameter) between the CPCR units and the tank were made of polyethylene tubing.

More details concerning the illuminated reactor areas A_R and the reactor volumes V_R, reflecting the number of photoreactors used in the different experimental runs, the total volume of the suspension V_S treated in each experiment, and the initial concentration of the pollutant (determined as TOC), are presented in Table 2.

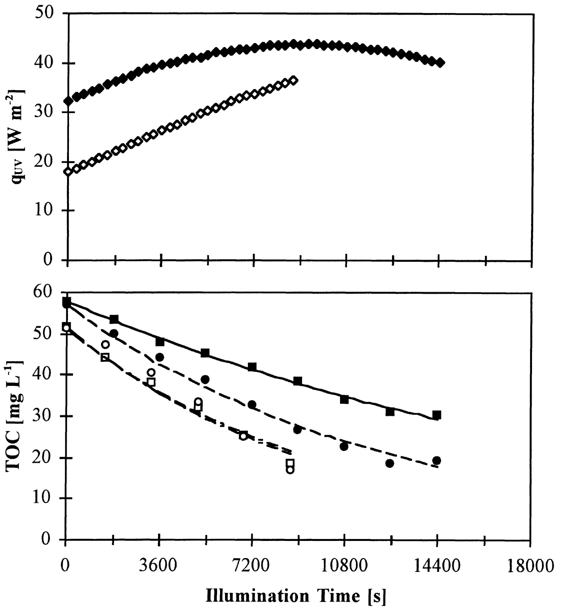

Fig. 2. Flux of UV energy and TOC versus illumination time during the outdoor experiments of the photocatalytic degradation of DCA at the PSA. The lines in the lower diagram have been calculated using Eq. (10) and the data given in Table 2. (Experimental conditions: 5.0 g l^{-1} P 25 (Run 28): (——■——) CPCR, (-----●-----) DSSR, (◆) corresponding UV flux; 5.0 g l^{-1} Hombikat UV 100 (Run 21): (-·-·-·□-·-·-·) CPCR, (-··—○··—··—) DSSR, (◇) corresponding UV flux.

In Fig. 2, typical experimental results of the photocatalytic degradation of DCA, using P 25, as well as Hombikat UV 100 slurries in the DSSR and the CPCR are shown. The corresponding global UV radiation q_{UV} in the 300–400 nm wavelength region is given in the same figure. In all cases, the TOC decreased significantly during the illumination with solar UV light. Using P 25 (5 g l^{-1}) as the photocatalyst in the DSSR and the CPCR, the TOC decreased within 240 min from the initial 56.8 mg l^{-1} to a final value of 19.2 mg l^{-1}, and from initial 57.8 mg l^{-1} to 30.4 mg l^{-1}, respectively. The respective decrease within 150 min was from 51.1 mg l^{-1} to 16.8 mg l^{-1}, and from 51.6 mg l^{-1} to 18.4 mg l^{-1} when Hombikat UV 100 (5 g l^{-1}) was used as the photocatalyst. These results confirm that Hombikat UV 100 is more active than P 25 as a photocatalyst for the degradation of DCA. Working with the DSSR configuration, and comparing the results obtained in Run Nos. 24 and 25, an increase of the apparent rate constant was observed again when the photonic absorption rate was decreased. The same effect was not equally observed using the CPCR arrangement.

Table 2

Experimental data and kinetic parameters (k_3) of the outdoor experiments at the PSA of the photocatalytic degradation of dichloro acetic acid[a]

Run No.	Catalyst	c_{cat} ($g\,l^{-1}$)	$\bar{q}_{UV}$ ($W\,m^{-2}$)	DSSR						CPCR						$k_{3,CPCR}/k_{3,DSSR}$
				V_S (l)	V_R (l)	A_R (m^2)	TOC_0 ($mg\,l^{-1}$)	$k_3 \times 10^8$ ($m^3\,W^{-1}\,s^{-1}$)	$\zeta \times 10^3$	V_S (l)	V_R (l)	A_R (m^2)	TOC_0 ($mg\,l^{-1}$)	$k_3 \times 10^8$ ($m^3\,W^{-1}\,s^{-1}$)	$\zeta \times 10^3$	
17	Hombikat UV 100	0.25	38.1	143	27.2	2.67	61.7	13.3 ± 1.5	234	159	35.4	2.97	55.5	11.9 ± 1.1	188	0.89
18	Hombikat UV 100	0.5	37.0	143	27.2	2.67	55.2	15.6 ± 1.7	245	159	35.4	2.97	47.2	15.1 ± 1.6	203	0.97
19	Hombikat UV 100	1.0	34.6	143	27.2	2.67	61.2	15.5 ± 1.9	270	159	35.4	2.97	49.7	15.1 ± 2.0	214	0.97
20	Hombikat UV 100	2.5	32.7	143	27.2	2.67	51.3	22.2 ± 1.6	324	159	35.4	2.97	43.0	23.4 ± 1.8	286	1.05
21	Hombikat UV 100	5.0	27.4	143	27.2	2.67	51.1	19.3 ± 1.9	281	159	35.4	2.97	51.6	20.3 ± 0.1	298	1.05
22	P 25	0.18	23.7	157	40.8	4.02	42.8	8.1 ± 0.3	99	–	–	–	–	–	–	–
23	P 25	0.25	23.7	–	–	–	–	–	–	248	10.6	8.91	55.3	10.3 ± 0.3	162	–
24	P 25	0.5	23.0	157	40.8	4.02	68.2	6.8 ± 0.4	132	220	70.8	5.94	55.3	7.2 ± 0.2	113	1.06
25	P 25	0.5	14.1	157	40.8	4.02	60.3	11.6 ± 0.4	199	220	70.8	5.94	55.1	6.8 ± 0.3	107	0.59
26	P 25	1.0	27.0	157	40.8	4.02	63.0	9.6 ± 0.1	172	220	70.8	5.94	55.8	9.3 ± 0.1	148	0.97
27	P 25	2.5	36.4	157	40.8	4.02	57.9	10.3 ± 0.5	170	220	70.8	5.94	53.7	8.4 ± 0.4	128	0.81
28	P 25	5.0	40.5	143	27.2	2.67	56.8	10.6 ± 0.3	171	159	35.4	2.97	57.8	6.2 ± 0.1	102	0.58

[a] Experimental conditions: DCA; pH 2.5; ambient temperature; DSSR: $\dot{V} = 12.0\,l\,min^{-1}$; CPCR: $\dot{V} = 33.3\,l\,min^{-1}$; Almería, Spain, 8–28 May 1996l

A whole series of experiments, similar to those presented in Fig. 2, have been performed in the DSSR and the CPCR using DCA as the model pollutant as well as different catalysts and concentrations (cf. Table 2). For these experimental runs performed at the PSA, initial photonic efficiencies varying from about 0.1 to about 0.2 for P 25, and from about 0.19 to about 0.3 for Hombikat UV 100 have been determined (cf. Table 2). These values are even higher than those reported for laboratory experiments using a 50 ml stirred tank reactor and artificial illumination [27]. When comparing photonic efficiencies calculated from the results of the experiments with the DSSR with those reported by Lindner et al. obtained under small-scale laboratory conditions [27], it should be noted that illumination intensities in the experiments reported here are significantly lower than in the experiments described in [27].

The lines in the lower part of Fig. 2 represent the exponential curve fits of the experimental data, calculated with the k_3 values provided by the parameter estimator, according to the rate law given in Eq. (10). As can be seen from these plots, this rate law yields a fairly good fit of the experimental data. More complete information is compiled in Table 2.

Under the experimental conditions employed at the PSA, the k_3 values obtained in the DSSR were higher (within the experimental error) than the values obtained in the CPCR in almost all cases. As expected, an influence of the catalyst type and its concentration on these k_3 values was observed. For both types of photoreactors, this dependence is graphically presented in Fig. 3. For comparison, k_3 values obtained in the laboratory experiments, reported in the foregoing section, are also presented in this figure.

The k_3 values for the degradation of DCA, obtained in the outdoor experiments at the PSA using Hombikat UV 100 as the photocatalyst, start at $13.3\times10^{-8}\,\mathrm{m^3\,W^{-1}\,s^{-1}}$ in the DSSR, and at $11.9\times10^{-8}\,\mathrm{m^3\,W^{-1}\,s^{-1}}$ in the CPCR at the lowest catalyst loading of $0.25\,\mathrm{g\,l^{-1}}$, increasing quickly up to about $23\times10^{-8}\,\mathrm{m^3\,W^{-1}\,s^{-1}}$ at a catalyst concentration of $2.5\,\mathrm{g\,l^{-1}}$, where maxima of the k_3 values are observed. In both types of photoreactors, the k_3 values decrease to about $20\times10^{-8}\,\mathrm{m^3\,W^{-1}\,s^{-1}}$ when the Hombikat UV 100 concentration is increased to $5\,\mathrm{g\,l^{-1}}$. This decrease of the kinetic parameter k_3 was not observed in the laboratory experiments using the DSSR under artificial illumination and catalyst concentrations up to $7.5\,\mathrm{g\,l^{-1}}$. The k_3 values for the degradation of DCA using P 25 as the photocatalyst start at $6.8\times10^{-8}\,\mathrm{m^3\,W^{-1}\,s^{-1}}$ in the DSSR and at $7.2\times10^{-8}\,\mathrm{m^3\,W^{-1}\,s^{-1}}$ in the CPCR at a catalyst loading of $0.5\,\mathrm{g\,l^{-1}}$, increasing quickly up to a catalyst concentration of $1–2.5\,\mathrm{g\,l^{-1}}$ to reach a maximum value of about $10\times10^{-8}\,\mathrm{m^3\,W^{-1}\,s^{-1}}$. The subsequent increase of the k_3 values above this catalyst loading is much slower. In the CPCR, k_3 even decreases to about $6\times10^{-8}\,\mathrm{m^3\,W^{-1}\,s^{-1}}$ at a catalyst concentration of $5\,\mathrm{g\,l^{-1}}$. This behavior is similar to that observed in the laboratory experiments with the DSSR, and in experiments with a small-scale photoreactor [27].

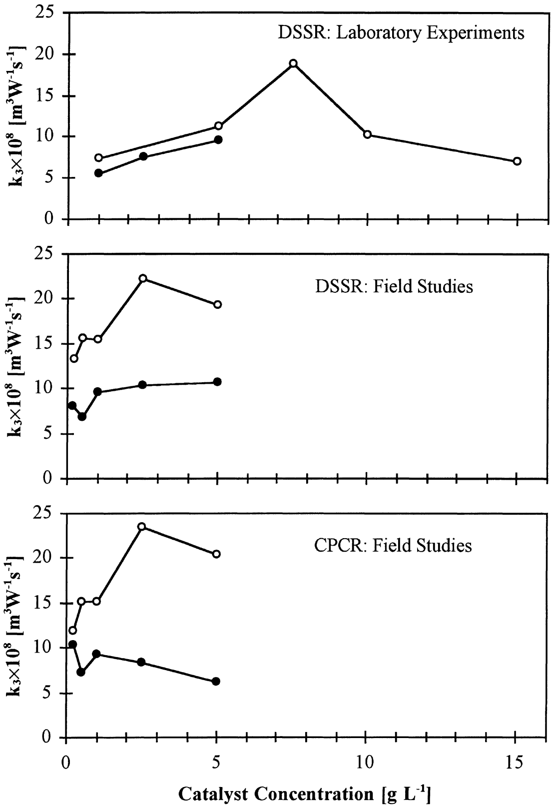

Fig. 3. Influence of the photocatalyst and its concentration on the kinetic parameter k_3 (○) Hombikat UV 100; (●) P 25).

Comparing the k_3 values obtained with the DSSR during the outdoor experiments at the PSA and the foregoing laboratory studies in Hannover, a fairly good agreement is observed when Degussa P 25 was used (see, for example, runs performed with a catalyst concentration of 5 g l^{-1}). It should be noted that these runs were carried out at very similar irradiation rates (40.5 and 38.5 W m^{-2}, respectively). With Sachtleben Hombikat UV 100, however, and comparing data for the same catalyst concentrations (5 g l^{-1}), such an agreement does not exist. A difference by a factor of 2 was observed. A partial explanation is clear: irradiation rates were very different (27.4 and 38.5 W m^{-2}, respectively), and, as pointed out before, k_3 values exhibit a definitive increasing trend when radiation fluxes are decreased. However, unless some disguised experimental failure is present, this argument is not sufficient to explain the differences of the results observed in Run Nos. 1 and 19.

In Table 2, the ratio $k_{3,\mathrm{CPCR}}/k_{3,\mathrm{DSSR}}$ is also given. This ratio, which reflects the different ability of the photoreactors to utilize the available light, is (within experimental error) smaller than 1 in almost all cases. Thus, it can be concluded that the DSSR is slightly more efficient than the CPCR in utilizing the solar radiation impinging on the reactor surface. It is known that in the spectral range from 295 to 387 nm, the reflection efficiency of polished aluminum used for the reflectors of the CPCR, is 83.2%. The transmissivity of the Teflon pipes in the spectral range under consideration is 76.8% [29]; so, at the most 63.9% of the total UV light falling on the reflecting surface can be utilized in the reaction pipe of the CPCR. However, with a few exceptions, the observed results are not showing such a high decrease in efficiency of the CPCR, as compared with the DSSR. Two arguments can explain this result: (i) back-scattering losses that are much more significant in the flat-plate configuration of the DSSR, and (2) a more effective turbulent flow regime (Re $\approx$ 15,000) used in the CPCR resulting in more favorable mixing conditions for catalyst activation and catalyst surface oxygenation.

4. Experiments with biologically pretreated industrial wastewater

4.1. Laboratory studies

The promising results of the photocatalytic degradation experiments with the model pollutant DCA obtained in the DSSR encouraged us to investigate the photocatalytic degradation of organic compounds present in biologically pretreated effluents. Samples from Volkswagen AG production plants in Wolfsburg (Germany) and Taubaté (Brazil) were tested using the DSSR and artificial UV light in the laboratory [13,14]. In these laboratory experiments, P 25, Hombikat UV 100, and a self-prepared platinized Hombikat UV 100 [32] were used as photocatalysts. In all experiments, the catalyst concentration was adjusted to 5 g l^{-1}. The experimental setup comprised one DSSR (modified SDP 16/32, Röhm GmbH, Darmstadt) either with $A_R = 1.34\,m^2$ and $V_R = 14.4\,l$, or with $A_R = 0.67\,m^2$ and $V_R = 7.2\,l$, which was connected to a tank with a pipe forming the loop of a recirculating batch system. The reactor was illuminated with the custom-made illumination unit described above. The averaged energy flux $\bar{q}_{UV}$ was 45 W m^{-2}, as determined by a luxmeter. In some experiments, the surface of the photoreactor was covered with a commercially available polymer sheet, thus lowering the available energy flux. In two experiments, the reactor surface was covered to exclude all light from the illumination unit, except for a window with an area of $50 \times 50\,cm^2$ ($A_R = 0.25\,m^2$, $V_R = 3.1\,l$). The suspension ($V_S = 10\,l$ or $20\,l$) was recirculated with a flow rate of 17 l min^{-1} by means of a centrifugal pump. To investigate the cleaning-up of greater amounts of wastewater, two experiments were performed employing three DSSR units connected in series (modified SDP 16/32; $A_R = 4.02\,m^2$, $V_R = 43.2\,l$), and adjusted to an inclination angle of 45°. The reactors were illuminated with solar light or with three illumination units (Solarien H 541, Philips, each equipped with eight UV-A lamps Cleo Performance 100 W). In these experiments, the suspension ($V_S > 200\,l$) was recirculated with a flow rate of 5 l min^{-1}.

More experimental data, and the values calculated for the kinetic parameter k_3 are compiled in Table 3. As can be seen from this table, the k_3 values obtained in these experiments vary between 0.5×10^{-8} and $21.0 \times 10^{-8}\,m^3\,W^{-1}\,s^{-1}$.

It should be noted that the discussion of these results is complicated by the fact that different real wastewater samples were used in this study. Thus, the initial TOC was not always the same (cf. Table 3), and, to some extent, the chemical nature and surely the concentrations of the pollutants present in the water changed

Table 3
Experimental data and kinetic parameters (k_3) of the laboratory experiments of the photocatalytic treatment of a biologically pretreated industrial wastewater[a]

Run No.	Catalyst	$\bar{q}_{UV}$ (W m^{-2})	V_S (l)	V_R (l)	A_R (m^2)	TOC$_0$ (mg l^{-1})	$k_3 \times 10^8$ (m^3 W^{-1} s^{-1})
29	Hombikat UV 100	45	20	14.4	1.34	8.2	0.80
30	Hombikat UV 100, platinized	45	20	14.4	1.34	12.8	1.4 ± 0.2
31	P 25	45	20	14.4	1.34	9.2	0.5 ± 0.0
32	P 25	45	10	7.2	0.67	5.5	3.1 ± 0.2
33	P 25	45	10	7.2	0.67	4.8	4.4 ± 0.3
34	P 25	45	10	7.2	0.67	6.9	5.1 ± 1.4
35[b]	P 25	45	20	14.4	1.34	9.0	2.5 ± 0.2
36[c]	P 25	3.9	20	14.4	1.34	7.9	8.7 ± 1.9
37	P 25	45	20	3.1	0.25	6.8	11.8 ± 1.8
38	P 25	22.5	20	3.1	0.25	7.0	21.3 ± 1.4
39[d]	P 25	33.4	230	43.2	4.02	7.9	7.7 ± 0.2
40[d,e]	P 25	18.5	280	43.2	4.02	9.3	9.1 ± 0.9

[a] Experimental conditions: biologically pretreated industrial wastewater; $c_{cat} = 5$ g l^{-1}; natural pH; ambient temperature; $\dot{V} = 17$ l min^{-1}.
[b] Oxygenated suspension.
[c] Solar experiment (Hannover, Germany, 28 August 1997, 9:45 a.m.–3:45 p.m.).
[d] $\dot{V}$ 5 l min^{-1}.
[e] Solar experiment (Hannover, Germany, 9 September 1997, 11:30 a.m.–4:30 p.m.).

from one sample to the next. It is well known that the photocatalytic degradation rate depends on the chemical structure of the existing pollutants.

This effect is apparent while analyzing the results obtained in Runs 32–34, which were performed under the same operating conditions, except for the initial TOC. The influence of the wastewater constituents on the value of the parameter k_3 is clearly observed. (cf. Table 3). Moreover, comparing the results of Run Nos. 33 and 34 with the oxygenated suspension (Run No. 35), it seems clear that in some cases the effect of the liquid composition may even prevail over that expected from a better-oxygenated catalyst. In spite of the limitations resulting from undefined pollutant concentrations, some qualitative observations and well-defined trends can be derived from this simple analysis of the experimental results.

The effect of decreasing the irradiation rates is clearly observed in Run Nos. 36, 38, and 40. Effects described in previous sections are also clearly observed here. When the DCA experiments were analyzed, the need for a better account of the existing oxygen concentration in the reaction volume (illuminated reactor) became apparent. This effect is also qualitatively observed in these runs: comparing Run No. 34 with Run No. 37, the dioxygen concentration decreased from an initial value of 8.6 mg l^{-1} to a final value of 2.9 mg l^{-1} within 3 h in the first case, and from initially 6.9 mg l^{-1} to a final value of 4.2 mg l^{-1} after 7 h of illumination in the second case. Consequently, the kinetic parameter for Run No. 37 is calculated to be more than two times larger than that of Run No. 34. A similar effect is obvious when Run Nos. 38 (Re ≅ 13,000) and 40 (Re ≅ 4000) are compared. The more favorable mixing conditions for catalyst activation and catalyst surface oxygenation in the first case lead to an increase in the observed kinetic parameter by more than a factor of two.

Using the k_3 values obtained in these experiments, the reactor area A_R necessary for the treatment of a suspension volume V_S can be calculated by Eq. (13):

$$A_R = \frac{V_S \ln(c_0/c)}{k_3 \bar{q}_{UV} t} \tag{13}$$

which is derived after rearrangement of Eq. (11). Using this equation and $V_S = 1$ m^3, $k_3 = 12 \times 10^{-8}$ m^3 W^{-1} s^{-1}, and $\bar{q}_{UV} = 20$ W m^{-2}, it can be calculated that an illuminated reactor area of 33 m^2 will be necessary to degrade 90% of the TOC, initially present in the wastewater, within 8 h ($t = 28\,800$ s) of illumination.

4.2. Pilot plant studies

Since the practical results of the laboratory studies mentioned above were promising, a pilot plant for the solar catalytic treatment of a biologically pretreated industrial wastewater was constructed. At its final location at the automobile production plant in Taubaté (VW do Brasil, Brazil), this pilot plant should reduce the TOC of pretreated wastewater from an initial concentration of about 10 mg l^{-1} to a final concentration of less than 1 mg l^{-1}, when charged with 0.5 m^3 wastewater per day.

The pilot plant consists of twelve double-skin sheet photoreactors (SDP 16/32, Röhm GmbH, Darmstadt, manufactured by Solacryl Gesellschaft für regenerative Energiesysteme mbH, Elsenfeld), which are adjusted to an inclination angle of 23° (corresponding to the latitude of Taubaté) facing south. Two DSSR units are connected in series, forming one reactor line. A recirculation pipe (approx. volume, 1.1 m^3) connects to a reservoir six of these lines running in parallel. The light harvesting reactor area of a single DSSR is $245 \times 94\,cm^2$ resulting in a total irradiated area $A_R = 27.6\,m^2$ and a total reactor volume $V_R = 301\,l$. Water ($V_{in} = 500\,l$) coming from the biological treatment plant is pumped into the reservoir. The solar catalytic treatment starts after the reservoir has been filled. The suspension ($V_S = 1011\,l$) is pumped by a centrifugal pump from the reservoir into the photoreactors and back through a reflux pipe into the reservoir for the desired illumination time during the day.

For the experiments described below, the flow rate out of the tank was varied between 83.3 and 133 l min^{-1}, resulting in a flow rate between 13.9 and 22.2 l min^{-1} in the reactor sheets. In some experiments, only six DSSRs, with $A_R = 13.8\,m^2$, $V_R = 151\,l$, and $V_S = 861\,l$, were used. After the desired time of the solar catalytic wastewater treatment, the recirculation pump was switched off and the water was pumped out of the reactors and back into the reservoir. The photocatalyst (5 g l^{-1}, Degussa P 25) settled down in the reservoir during the night. When sedimentation was over, the supernatant liquid ($V_{out} = 500\,l$) was pumped out of the reservoir.

To test the performance of this pilot plant, it has been installed at the production plant of Volkswagen AG in Wolfsburg (Germany) in May 1998. Fig. 4 shows the results of a typical experimental run.

The variability of the UV(A)-intensity shown at the top of Fig. 4 gives a clear indication of the usual operating conditions of a solar plant. Hence, in addition to the difficulties of handling a liquid of variable and not well-known composition, the solar fluxes exhibit significant variations during the course of the day. Variations of ±50% around the mean are by no means unusual.

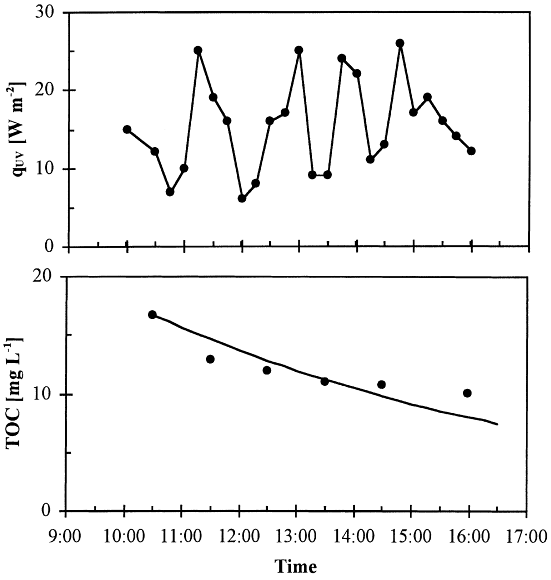

Fig. 4. Flux of UV energy and TOC versus time during the photocatalytic treatment of biologically pretreated industrial wastewater in the pilot plant. The lines in the lower diagram have been calculated using Eq. (10) and the data given in Table 4 (Run 47).

The TOC values of the incoming wastewater were determined to vary between 10.2 and 26.9 mg l^{-1}. The wastewater was slightly alkaline (pH 7.6 ± 0.2); the initial dioxygen concentration was 8.5 ± 1.4 mg l^{-1}. By mixing the incoming wastewater with the catalyst slurry that remained in the pilot plant after the supernatant water treated during the previous day was pumped out, the TOC decreased to initial values varying between 7.3 and 26.9 mg l^{-1}.

During the solar catalytic treatment, a decrease in the concentration of the organic pollutants, determined as TOC, was observed in all cases. As an example, the changes in TOC during a single run of the pilot plant are given in the lower part of Fig. 4. As can be seen from this figure, the TOC decreased from an initial value of 16.7 mg l^{-1} to a final value of 10.0 mg l^{-1} within 330 min of solar illumination. The time averaged energy flux was 13.3 W m^{-2} (with minimum and maximum peaks of 6 and 26 W m^{-2} approximately).

Table 4
Experimental data and kinetic parameters (k_3) of the pilot plant experiments of the photocatalytic treatment of biologically pretreated industrial wastewater[a]

Run No.	c_{cat} (g l^{-1})	$\dot{V}$ (l min^{-1})	$\bar{q}_{\mathrm{UV}}$ (W m^{-2})	V_{S} (l)	V_{R} (l)	A_{R} (m^2)	TOC$_0$ (mg l^{-1})	$k_3 \times 10^8$ (m^3 W^{-1} s^{-1})
41	2.5	16.7	27.4	1011	301	27.6	29.1	9.9 ± 7.8
42	2.5	16.7	22.4	1011	301	27.6	14.9	5.8 ± 3.7
43	2.5	16.7	22.8	1011	301	27.6	15.4	7.8 ± 5.2
44	2.5	16.7	19.1	1011	301	27.6	10.2	4.0 ± 0.9
45	5	13.9	17.6	1011	301	27.6	10.4	6.1 ± 2.0
46	5	13.9	6.8	1011	301	27.6	11.8	3.5 ± 0.5
47	5	19.4	13.3	1011	301	27.6	16.7	10.2 ± 4.4
48	5	19.4	18.1	1011	301	27.6	13.1	2.5 ± 1.2
49	5	16.7	17.7	861	151	13.8	7.1	7.9 ± 2.0
50	5	16.7	26.7	861	151	13.8	9.4	2.8 ± 0.9
51	5	22.2	26.0	861	151	13.8	12.9	4.6 ± 1.3
52	5	22.2	26.1	861	151	13.8	10.2	6.1 ± 0.8
53	5	13.9	24.6	861	151	13.8	12.1	2.1 ± 0.6
54	5	13.9	15.2	861	151	13.8	13.3	5.1 ± 4.9
55	5	13.9	10.8	861	151	13.8	12.6	6.7 ± 3.3
56	5	13.9	13.0	861	151	13.8	17.0	2.1 ± 1.0
57	5	13.9	24.5	861	151	13.8	11.7	0.7 ± 0.3

[a] Experimental conditions: biologically pretreated industrial wastewater; TiO_2 Degussa P 25; natural pH; ambient temperature; Wolfsburg, Germany, 15 May–20 July 1998.

In this run, 85% of the totally eliminated organic carbon was photocatalytically degraded within the first 180 min of irradiation. As a consequence of this oxidation process as well as due to the increase in the reaction temperature, the dioxygen concentration in the suspension, measured in the reflux pipe (between the photoreactors and the tank) and inside the tank, decreased from 8.8 and 8.0 mg l^{-1}, respectively, to 7.0 and 6.5 mg l^{-1}, respectively. This decrease in the dioxygen concentration, as well as a decrease in the concentration of inorganic carbon (IC: CO_2, ${CO_3}^{2-}$, ${HCO_3}^{-}$) was observed in all experimental runs performed with the pilot plant in Wolfsburg. In most runs, the pH of the suspension increased by 0.3 to 1.3 pH units. In the particular run shown in Fig. 4, the pH of the suspension increased from an initial value of 7.8 to a final value of 8.3.

More than 50% of the organic pollutants initially present in the mixed water inside the pilot plant can, thus, be degraded within 8–11 h of illumination. Naturally, the total mass of the degraded contaminants will depend on the initial pollutant composition and concentration, the time of illumination and on the available solar UV flux.

The k_3 values calculated for the TOC reduction from all experimental runs, which have been analyzed in detail, are summarized in Table 4, together with the relevant experimental details.

Leaving aside results associated with an error limit for the determination of the parameter estimator exceeding 40%, the values of k_3 are found to vary between 2×10^{-8} and 6×10^{-8} m^3 W^{-1} s^{-1}. The value of about 12×10^{-8} m^3 W^{-1} s^{-1}, observed in an experiment with artificial UV light and used for the calculation of the required reactor area for the treatment of 1 m^3 of wastewater (vide supra), was not reached in any of these solar experimental runs. The observed variations of the values of k_3 cannot be correlated with the COD, TOC, or IC (CO_2, ${CO_3}^{2-}$, ${HCO_3}^{-}$) of the incoming wastewater, nor with the pH, the concentration of molecular oxygen dissolved in the suspension, the mean UV light intensity during the day, the time of illumination or the flow rate.

These variations might be mainly due to differences in the compounds actually present in the wastewater, which have not been determined analytically. As mentioned above, it is well known that the reaction rate of the photocatalytic degradation of organic wastewater pollutants depends strongly on their chemical nature, and it is expected that the values obtained for the kinetic parameter k_3 will reflect this fact.

In some runs (Run Nos. 45, 46, 47, and 49) a leveling-off of the TOC disappearance was observed. Such an effect could, for example, be explained by the presence of some compounds of high molecular weight that may be mineralized in a multi-step oxidation process. This was concluded from the following observations: (i) while the TOC remained nearly constant, the COD further decreased under solar irradiation, and (ii) in all cases when this behavior was observed, the photocatalytic degradation process on the following day, employing a new batch of wastewater, but using the same catalyst, was not affected.

In any event, considering all the previously stated limitations of the approximate model, as well as the described difficulties of performing solar experiments with real wastewaters, it should be taken as a confirmation of this model's validity that all calculated kinetics parameters are found to be within the same order of magnitude (cf. Table 4).

5. Conclusions

The results reported above clearly demonstrate the practical applicability of the double-skin sheet reactor (DSSR) for the use in solar water treatment. It was shown that this type of photoreactor offers an interesting alternative for solar catalytic water detoxification plants, especially because its basic components are readily available industrially.

Using DCA as the model pollutant, an excellent qualitative and, in some cases, quantitative agreement between the results from the studies described here and previous laboratory experiments performed with a 50 ml stirred-tank reactor has been observed.

A newly derived pseudo first-order rate law in pollutant concentration and apparent irradiation rate (Eq. (8)) can be used to analyze the experimental data obtained with artificial UV illumination with a constant flux of photons, as well as under fluctuating radiation conditions in solar outdoor experiments. The model has a single parameter that can be estimated from these experiments (Eq. (11)). After integration and rearrangement, the rate law can be used for an approximate scaling-up of a pilot plant for solar catalytic wastewater treatment.

Results with the model pollutant DCA indicate that the main variables that affect the defined single kinetic parameter are (i) the concentration of molecular oxygen, (ii) the type of photocatalyst, (iii) the catalyst loading, and (iv) the irradiation level. The model does not account for the first three parameters. Furthermore, the last parameter, included in the model in form of a linear dependence, does not seem to be useful for extrapolating significant changes in the irradiation rates.

However, the derived expression has proved to be a valid tool for comparing performances of different photocatalytic reactors under equivalent operating conditions.

Therefore, it seems reasonable to use a sequential method for future scale-ups. As a first step, using real wastewaters, laboratory experiments should be performed changing the kind and the concentration of the photocatalyst. A k_3 value for a given catalyst and catalyst concentration, calculated from these experiments, should be used to approximate the illuminated reactor area A_R required for the treatment of a suspension volume V_S. The latter conditions should then be used in subsequent bench-scale experiments employing solar irradiation. These experiments must maintain the type of photocatalyst and the catalyst concentration previously selected. The resulting value of the kinetic parameter k_3 obtained from this second set of experiments can be applied for the proper designing of a solar catalytic wastewater treatment plant having the same reactor thickness, similar hydrodynamic operating conditions and oxidant concentrations.

We are optimistic that the design of future solar water treatment plants can be based upon the scale-up of results obtained with such a small set of laboratory experiments.

6. Nomenclature

A_R	total illuminated (light-harvesting) surface area of the photoreactor(s) (m^2)
c	concentration ($g\,m^{-3}$ or $mol\,m^{-3}$)
$\langle e^a \rangle_{V_R}$	volume averaged photon absorption rate (Einstein $m^{-3}\,s^{-1}$)
$\langle \langle e^a \rangle_{V_R} \rangle_\tau$	time averaged and volume averaged photon absorption rate (Einstein $m^{-3}\,s^{-1}$)
k_λ	constant ($k_\lambda = 8.359$ Einstein $W^{-1}\,s^{-1}\,m^{-1}$)

$k^*_\lambda = k_\lambda \times \lambda$	the conversion factor from W to Einstein s^{-1} at a given λ (Einstein $\mathrm{W}^{-1}\,\mathrm{s}^{-1}$)
k_1	kinetic constant (Eq. (3)) (m^3 $\mathrm{Einstein}^{-1}$)
$k_2 = k_\lambda \times \lambda$	the conversion factor from W to Einstein s^{-1} for $\lambda = 350 \times 10^{-9}$ m (Einstein $\mathrm{W}^{-1}\,\mathrm{s}^{-1}$)
$k_3 = k_1 k_2 \alpha$	kinetic parameter ($\mathrm{m}^3\,\mathrm{W}^{-1}\,\mathrm{s}^{-1}$)
q_λ	density flux of photons with wavelength λ per unit area and unit time (Einstein $\mathrm{m}^{-2}\,\mathrm{s}^{-1}$)
q_{UV}	density flux of UV energy per unit area and unit time ($\mathrm{W\,m}^{-2}$)
$q_{\mathrm{UV},\lambda}$	density flux of UV energy with wavelength λ per unit area and unit time ($\mathrm{W\,m}^{-2}\,\mathrm{s}^{-1}$)
$\bar{q}_{\mathrm{UV}}$	time averaged density flux of UV energy per unit area and unit time ($\mathrm{W\,m}^{-2}$)
R_{V}	reaction rate per unit suspension volume ($\mathrm{mol\,m}^{-3}\,\mathrm{s}^{-1}$)
t	time (s)
V_{R}	total illuminated volume of the photoreactor(s) (m^3)
V_{S}	total volume of suspension (m^3)
$\dot{\mathrm{V}}$	flow rate ($\mathrm{m}^3\,\mathrm{s}^{-1}$)
α_λ, α	factor reflecting the ability of a photoreactor to use the available light
ζ	photonic efficiency (moles $\mathrm{Einstein}^{-1}$)
λ	wavelength (m)

Acknowledgements

The photocatalytic experiments mentioned in this article have been performed by M. van Well, H.-W. Schumacher, M. Schober, S. Vollmer, and E. Gross. Their contributions are gratefully acknowledged. We thank G. Hocke, M. Rimpl, and R. Sättler (Röhm GmbH Chemische Fabrik, Darmstadt, Germany) for the fabrication of the double-skin sheet reactors. The work at the Plataforma Solar de Almería has been financed by the EC in the frame of the EC-program DGS XII 'Training and Mobility for Researchers (TMR)' under contract No. ERBMFG-CT95-0023 (Innovative Training Horizons in Applied Thermal and Chemical Technologies). This financial support is gratefully acknowledged here. The authors wish to thank J. Blanco, S. Malato, and C. Richter for their kind and helpful support for using the facilities at the Plataforma Solar de Almería. Parts of the work were performed on behalf of the Röhm GmbH Chemische Fabrik, Darmstadt, and of the Volkswagen AG, Wolfsburg (Germany). The authors wish to thank V. Benz (Röhm GmbH), K. Pahlmann, J. Wienefeld, and G. Sager (all Volkswagen AG) for their kind support and for many helpful discussions. A.E.C. thanks the Cooperation Program between Germany and Argentina, the Alexander von Humboldt Foundation, CONICET and the Universidad Nacional del Litoral for facilitating his participation in this project.

References

[1] M.R. Hoffmann, S.T. Martin, W. Choi, D.W. Bahnemann, Chem. Rev. 95 (1995) 69.
[2] D. Bahnemann, in: P. Boule (Ed.), Environmental Photochemistry [The Handbook of Environmental Chemistry, 2L], Springer, Berlin, 1999, p. 285.
[3] R.E. Bird, R.L. Hulstrom, L.J. Lewis, Solar Energy 30 (1983) 563.
[4] D. Bahnemann, D. Bockelmann, R. Goslich, Dechema Monogr. 124 (1991) 261.
[5] D.Y. Goswami, in: K.W. Boer (Ed.), Advances in Solar Energy 10, American Solar Energy Society, Boulder, CO, 1995, p. 165.
[6] D.Y. Goswami, ASME J. Solar Energy Eng. 119 (1997) 101.
[7] K. Pacheco, A.S. Watt, C.S. Turchi, in: A. Kirkpatrick, W. Worek (Eds.), ASME/ASES Joint Solar Energy Conference, ASME, New York, NY, 1993, p. 43.
[8] C.S. Turchi, M.S. Mehos, in: 2nd Int. Symp. on Chemical oxidation: technology for the nineties, Technomic Publishing Company, Lancaster, PA, 1994, p. 301.
[9] R.J. Brandi, O.M. Alfano, A.E. Cassano, J. Adv. Oxid. Technol. 3 (1998) 213.
[10] M. van Well, R.H.G. Dillert, D.W. Bahnemann, V.W. Benz, M.A. Müller, ASME J. Solar Energy Eng. 119 (1997) 114.
[11] R. Dillert, R. Goslich, J. Dzengel, H.-W. Schumacher, D. Bahnemann, in: D. Martínez (Ed.), Proc. 1st users workshop training and mobility of researchers programme at Plataforma Solar de Almería, Editorial CIEMAT, Madrid, 1998, p. 31.
[12] D. Bahnemann, R. Dillert, J. Dzengel, R. Goslich, G. Sagawe, H.-W. Schumacher, V. Benz, J. Adv. Oxid. Technol. 4 (1999) 11.
[13] R. Dillert, S. Vollmer, M. Schober, J. Theurich, D. Bahnemann, H.-J. Arntz, K. Pahlmann, J. Wienefeld, T. Schmedding, G. Sager, Chem. Eng. Technol. 71 (1999) 396.
[14] R. Dillert, S. Vollmer, M. Schober, J. Theurich, D. Bahnemann, H.-J. Arntz, K. Pahlmann, J. Wienefeld, T. Schmedding, G. Sager, gwf Wasser-Abwasser 140 (1999) 293.

[15] R. Dillert, S. Vollmer, E. Gross, M. Schober, D. Bahnemann, H.-J. Arntz, K. Pahlmann, J. Wienefeld, T. Schmedding, G. Sager, Z. Physikal. Chem., 1999 (in press).
[16] O.M. Alfano, R.J. Brandi, G. Sagawe, A.E. Cassano, unpublished results.
[17] M.I. Cabrera, O.M. Alfano, A.E. Cassano, J. Phys. Chem. 100 (1996) 20043.
[18] J. Blanco, S. Malato, Tecnologia De Fotocatalisis Solar — Utilizacion De La Radiacion Solar Para El Tratamiento De Contaminantes Industriales, Almeria, Spain, Institio de Estudios Almerienses de la Diputacion de Almeria CIEMAT, 1996.
[19] M.S. Mehos, K.A. Pacheco, H.F. Link, in: W.B. Stine, J. Kreider, K. Watanabe (Eds.), ASME International Solar Energy Conference, ASME, New York, NY, 1992, p. 51.
[20] G. Sagawe, Ph.D. Thesis, University of Clausthal, 1999, in preparation.
[21] G. Sagawe, R. Dillert, D. Bahnemann, in: IPS-12 12th Int. Conf. on photochemical conversion and storage of solar energy, Berlin, Germany, 9–14 August 1998, p. 3W15.
[22] O.M. Alfano, M.I. Cabrera, A.E. Cassano J. Catal. 172 (1997) 370.
[23] G.H. Rossetti, E.D. Albizzati, O.M. Alfano, Ind. Eng. Chem. Res. 37 (1998) 3592.
[24] D. Bahnemann, D. Bockelmann, R. Goslich, M. Hilgendorff, D. Weichgrebe in: D.F. Ollis, H. Al-Ekabi (Eds.), Photocatalytic purification and treatment of water and air (Trace metals in the environment 3), Elsevier, Amsterdam, 1993, p. 301.
[25] D. Bahnemann, D. Bockelmann, R. Goslich, M. Hilgendorff, in: G.R. Helz, R.G. Zepp, D.G. Crosby (Eds.), Aquatic and Surface Photochemistry, Lewis, Boca Raton, 1994, p. 349.
[26] D. Bockelmann, Solare Reinigung verschmutzter Wässer mittels Photokatalyse, Ph.D. Thesis, University of Clausthal, 1993, Cuvillier, Göttingen, 1994.
[27] M. Lindner, D.W. Bahnemann, B. Hirthe, W.-D. Griebler, ASME J. Solar Energy Eng. 119 (1997) 399.
[28] R.J. Brandi, O.M. Alfano, A.E. Cassano, J. Adv. Oxid. Technol. 4 (1999) 76.
[29] J. Blanco, S. Malato, private communication, 1993.
[30] S. Malato, J. Blanco, C. Richter, M. Vincent, Solar Energy 56 (1996) 401.
[31] S. Malato, J. Blanco, C. Richter, D. Curcó, J. Giménez, Water Sci. Technol. 35 (1997) 157.
[32] D. Bockelmann, M. Lindner, D. Bahnemann, in: E. Pelizzetti (Ed.), Fine Particles and Technology, NATO ASI Series 3, vol. 12, Kluwer, Dordrecht, 1996, p. 675.